Am J Cancer Res 2023;13(7):3123-3139
www.ajcr.us /ISSN:2156-6976/ajcr0149847

Original Article

TPM3: a novel prognostic biomarker of cervical cancer that correlates with immune infiltration and promotes malignant behavior *in vivo* and *in vitro*

Yue-Chen Zhao[1], Tie-Jun Wang[1], Geng-Hui Qu[2], Li-Zhen She[1], Jie Cui[1], Rui-Feng Zhang[1,3], Hong-Dao Qu[1]

[1]*Department of Radiation Oncology, The Second Hospital of Jilin University, Changchun 130041, Jilin, P. R. China;* [2]*Department of Radiology, Dongliao County People's Hospital, Liaoyuan 136299, Jilin, P. R. China;* [3]*Department of Internal Medicin-1, Jilin Cancer Hospital, Changchun 130103, Jilin, P. R. China*

Received February 24, 2023; Accepted May 19, 2023; Epub July 15, 2023; Published July 30, 2023

Abstract: Cervical squamous cell carcinoma and endocervical adenocarcinoma (CESC) has become increasingly prevalent in younger women. Tropomyosin 3 (TPM3), a thin filament actin-binding protein, has been implicated in various malignancies. In this study, TPM3 expression was evaluated using RNA-seq data from The Cancer Genome Atlas (TCGA), and its relationship with CESC prognosis was examined with receiver operating characteristic (ROC) curves. The effects of TPM3 on cellular proliferation and migration were examined in CESC cell lines using Cell Counting Kit-8 (CCK-8), colony formation, and Transwell assays, while *in vivo* effects were assessed in mouse xenograft models. Furthermore, differentially expressed genes (DEGs) associated with TPM3 were investigated to determine their tumorigenic functions. Associations between TPM3, chemosensitivity, and immune infiltration were analyzed, as were links between mutations, methylation, and prognosis using the cBioPortal and MethSurv databases. Upregulation of TMP3 mRNA and protein levels was observed in CESC samples, with elevated mRNA levels associated with reduced overall survival. TPM3 showed an area under the curve (AUC) of 0.946 for CESC diagnosis and was found to regulate tumor proliferation and metastasis *in vitro* and *in vivo*. Overall, 3099 DEGs were identified and found to be enriched in key CESC progression-related signaling pathways. TPM3 expression was also correlated with intratumoral immune cell infiltration and immune checkpoint activity. Patients with higher TPM3 expression showed distinctive chemosensitivity profiles, and TPM3 gene methylation was linked to poorer CESC patient prognostic outcomes. In conclusion, TPM3 is a key regulator of CESC progression, prognosis, and the tumor immune microenvironment, suggesting its potential as a diagnostic or prognostic biomarker and target for CESC immunotherapy.

Keywords: Tropomyosin 3 (TPM3), cervical neoplasms, prognosis, tumour microenvironment, DNA methylation, epithelial-mesenchymal transition

Introduction

Cervical cancer (CC) is the fourth most common female malignancy with significant mortality and thus presents a substantial health challenge throughout the world [1]. Data from the International Agency for Research on Cancer indicate 604000 new CC cases in 2020, together with 342000 CC-related deaths, with 90% of deaths occurring in low-to-middle income countries [2, 3]. Despite the protective benefits of the human papillomavirus (HPV) vaccine for CC, regional disparities indicate that CC will continue to pose a severe health concern in the upcoming decades. The drive to facilitate personalized treatment and evaluate patient prognosis has sparked an intensified focus on identifying potential biomarkers that could predict treatment outcomes and survival rates. By linking the invasive clinical phenotype of the tumor to its gene expression profile, molecular markers with prospective prognostic utility can be identified.

Tropomyosin (TPM) is an actin-binding protein that is expressed in thin muscle filaments. It plays an important role in regulating muscle contraction and is widely distributed in various eukaryotic cells [4]. TPM3 is a member of the TPM family and encodes 284 amino acid pro-

teins expressed in both fibroblasts and slow-contracting skeletal muscles. TPM3 is involved in the stability of cytoskeletal microfilaments and binds to actin in muscle cells to regulate muscle contraction. In non-muscle eukaryotic tissues, actin microfilaments participate in various functions involving different actin structures, such as stress fibers, petal fibers, silk feet, contractile rings, and microvilli, contributing to cell movement, intracellular vesicle transport, and other cellular processes [5, 6].

Recent research has found that structural variations and changes in the expression levels of the TPM3 gene are correlated with the occurrence and development of various malignant tumors [7]. TPM3 plays various roles in many cellular signaling pathways, including the epithelial-mesenchymal transition (EMT), gene fusion, and PI3K/AKT signaling pathways [8]. Recent studies have also shown a significant association between TPM3 expression and the progression and prognosis of various tumors, including liver, lung, colon, esophageal and mesenchymal tumors [9-12]. Nevertheless, the association between TPM3 and cervical squamous cell carcinoma and endocervical adenocarcinoma (CESC) has not been investigated and still requires further exploration.

Data from The Cancer Genome Atlas (TCGA) were analyzed to gain insight into the prognostic and diagnostic implications of TPM3 expression and its functional role in CESC. The findings were verified by both *in vitro* and *in vivo* analyses. Correlations between TPM3 expression and parameters such as chemosensitivity, immune checkpoint expression, and immune cell infiltration were also evaluated. Together, these analyses will provide a sound basis for subsequent studies to clarify the role of TPM3 in CESC and its value as a diagnostic or therapeutic target in this cancer type.

Materials and methods

TCGA data

Data on patients with CESC were obtained from the TCGA database. The data included TPM3 mRNA expression levels and clinicopathological information such as patient age, TNM, and clinical staging.

Clinical sample collection

Paired samples of CESC tumor and adjacent healthy tissues were collected from patients undergoing surgery at The Second Hospital of Jilin University between January and August 2022. The patients had all been newly diagnosed with a clear pathological diagnosis of CESC and had not undergone any treatment before surgery. All human studies were approved by the Ethics Committee of The Second Hospital of Jilin University, and all participants provided written informed consent.

Immunohistochemical (IHC) analysis

An IHC kit (ThermoFisher, USA) was used, in accordance with the provided instructions. Briefly, 4-μm tissue sections were prepared, deparaffinized using xylene, rehydrated in an ethanol gradient, and treated with 3% H_2O_2. Antigen retrieval was subsequently conducted at room temperature (RT). Sections were blocked in 5% BSA for 0.5 h at RT, incubated overnight with an anti-TPM3 primary antibody (Abcam, UK) at 4°C, probed for 0.5 h with a secondary antibody, and visualized with DAB. The sections were then counterstained with hematoxylin, dehydrated in an ethanol gradient, fixed in neutral resin, and imaged under light microscopy.

Western immunoblotting

Tissues were lysed with RIPA buffer (Solarbio, China) and the proteins were separated on 10% SDS-PAGE (Beyotime, China) using a Bio-Rad electrophoresis system (USA) at 200 V for 40 minutes. The proteins were then transferred to PVDF membranes (Millipore, USA) at 400 mA for 30 minutes. Following blocking, the membranes were incubated overnight at 4°C with anti-TPM3 or anti-tubulin antibodies (Abcam, UK) and incubated for 2 h at RT with appropriate secondary antibodies. Visualization was done using a BeyoECL Plus Kit (Beyotime, China). The grayscale densities of the protein bands from the clinical samples were measured using ImageJ v1.8.0 to ascertain protein expression levels, with subsequent statistical analysis.

Cell culture and transfection

HeLa cells (Shanghai Institutes for Biological Sciences, Chinese Academy of Sciences) were cultured in DMEM (Hyclone, USA) containing 10% fetal bovine serum (FBS) (Gibco, USA) in a 5% CO_2 37°C incubator. TPM3 was knocked

down by transfection of cells with si-NC or si-TPM3 constructs (Genepharma, China) using Lipofectamine 3000 (Invitrogen, USA) and cultured for a further 48 h. The sequences of si-TMP3 were as follows: forward (F): 5'-UAAGAAUCUUGAUUUCUUCCU-3', reverse (R): 5'-GAAGAAAUCAAGAUUCUUACU-3'.

Real-time quantitative PCR (RT-qPCR) assays

Total RNA was extracted from transfected cells and xenograft tumors in all groups using TRIzol reagent (Tiangen, China), and cDNA was synthesized using a First Strand cDNA Synthesis Kit (TaKaRa Bio, Japan). RT-qPCR was performed on an ABI PRISM 7000 Sequence Detection System (Thermo Fisher, USA). The primer sequences for TPM3 were as follows: F: 5'-TGAAAACCGGGCCTTAAAAGAT-3', R: 5'-GATCACCAACTTACGAGCCAC-3'. GAPDH was used as an internal control, and the $2^{-\Delta\Delta CT}$ method was used for the calculation of the relative expression of TPM3 mRNA.

Cell counting kit-8 (CCK-8) assays

Following transfection, HeLa cells were seeded in 96-well plates (1×10^5 cells/mL) and allowed to grow for 48 h. Cell viability was measured with a CCK-8 kit (Meilunbio, China), according to the provided instructions, and absorbances at 450 nm were measured in a Bio-Rad model 550 microplate reader.

Colony-forming assays

Cells were seeded in 6-well plates (500 cells/well) and cultured for 48 h, after which they were treated with appropriate concentrations of ATO (2 μM for HeLa cells). After one week, the cells were fixed using 4% paraformaldehyde (Beijing Chemical Plant, China), stained with 2% crystal violet (Beyotime, China), and visible colonies (≥ 50 cells per clone) were counted under a microscope.

Wound-healing assay

After transfection, HeLa cells were grown to 80% confluence in 6-well plates, after which a straight scratch was generated with a pipette. Cells were imaged at 0 and 24 h post-wounding to measure migration using ImageJ software with the formula: cell migration index = (0 h scratch area - 24 h scratch area)/0 h scratch area.

Transwell assays

Transfected HeLa cells were added to the upper portion of Matrigel (Corning, USA)-coated Transwell inserts in serum-free media. MEM supplemented with 10% FBS was placed in the lower chamber. After incubation for 24 h, the invasive cells were fixed with 4% paraformaldehyde (Beijing Chemical Plant, China) and stained with Giemsa stain (Phygene, China). The invasive cells in five randomly selected fields of view were counted under light microscopy (100×).

In vivo xenograft model

All animal studies were approved by The Animal Care and Use Committee at the College of Basic Medicine of Jilin University and were conducted per NIH standards. A transfection kit (Genepharma, China) was used to transfect TMP3 shRNA (sh-TPM3) or the shRNA negative control (sh-NC) into HeLa cells to generate stably transfected cell lines. The sh-TMP3 sequences were as follows: F: 5'-CCGGCAAGATTCTTACTGATAAACTCTCGAGAGTTTATCAGTAAGAATCTTGTTTTTG-3'. Seven-week-old BALB/cA-nu mice (18-20 g) (Beijing Vital River Laboratory Animal Technology, China) received subcutaneous implanation of the transfected HeLa cells (1×10^7 cells/mouse). The sh-TPM3 and sh-NC groups included three mice each. After 27 days, the mice were euthanized, and the tumors were excised, imaged, and weighed. Tumor volumes were calculated as (length × width^2)/2. A 4% tissue fixative solution was used to fix tumors before hematoxylin & eosin (H&E) and IHC staining.

Identification and analysis of differentially expressed genes (DEGs)

DEGs related to TPM3 were identified using the LinkedOmics database and data from CESC patients in the TCGA database. The results were used to compile volcano plots, and DEGs were identified as genes exhibiting a fold-change > 1.5 and an FDR-corrected *P*-value < 0.05. A heatmap was additionally constructed by incorporating the 50 top up- and down-regulated DEGs. The functions of the DEGs were analyzed by Gene Ontology (GO) and Kyoto Encyclopedia of Genes and Genomes (KEGG) enrichment.

Assessment of immune infiltration

Single-sample Gene Set Enrichment Analysis (GSEA) was used to evaluate the infiltration of 24 types of immune cells and the expression of immune checkpoint molecules, including LAG3, CTLA4, TIGIT, SIGLEC15, HAVCR2, CD-274, PDCD1, and PDCD1LG2, using the "GSVA" package in R. The associations of immune infiltration and checkpoint expression with TPM3 expression in patients were analyzed.

Chemosensitivity analyses

The Genomics of Drug Sensitivity in Cancer database (https://www.cancerrxgene.org/) was used to predict the response of patients with CESC to chemotherapy using the R "pRRophetic" package. A ridge regression approach was used to calculate the half-maximal inhibitory concentration (IC_{50}) values for individual samples, with all analytical parameters at their default values.

Analysis of genetic alterations and methylation

Alterations in the TPM3 gene included in the TCGA (Firehose Legacy and PanCancer Atlas) database were assessed using cBioPortal (www.cbioportal.org). Differences in survival outcomes were compared with Kaplan-Meier plots and log-rank tests. The MethSurv database (biit.cs.ut.ee/methsurv/) was used to obtain data on methylation, and the association between the methylation of individual TPM3 CpG residues and survival was assessed.

Statistical analysis

All data in the study were the result of three replicates. R v3.6.1 was used for statistical analyses. Between-group comparisons were made with the Wilcoxon test, while receiver operating characteristic (ROC) curves were constructed with pROC software to assess the significance of TPM3 expression levels. Chi-square tests were used to analyze associations between TPM3 levels and clinical parameters in CESC patients. Overall survival (OS) was compared between groups using Kaplan-Meier curves and log-rank tests. Univariate and multivariate Cox regression analyses were used to assess prognostic indicators in CESC. Chemosensitivity was tested based on analyses of IC_{50} values. Bar graph and box plot error bars were used to indicate standard deviations (SDs). *P*-values < 0.05 were considered statistically significant.

Results

Assessment of the cancer expression profile of TPM3

TPM3 expression was initially assessed across all cancers in the TIMER 2.0 database, indicating its overexpression in BLCA, BRCA, CESC, CHOL, ESCA, HNSC, KIRC, KIRP, LIHC, LUAD, LUSC, STAD, THCA, and UCEC, and downregulation in COAD and KICH (**Figure 1A**). Higher TPM3 expression was evident in CESC patient tumors relative to healthy tissues ($P < 0.001$) (**Figure 1B**) and TPM3 expression was found to be correlated with clinical parameters, including histological tumor type and grade ($P < 0.05$) (**Figure 1C-I**). In contrast, TPM3 levels were found to be unrelated to patient age or tumor T, N, M, or clinical stages ($P > 0.05$). Both IHC and Western immunoblotting also confirmed the upregulation of TPM3 in tumors compared to corresponding control samples (**Figure 1J**, **1K**). Statistical analysis of Western immunoblotting revealed that the expression of TPM3 in tumor samples was higher than that in control samples ($P < 0.0001$) (**Figure 1K**), in line with the TCGA database results.

Assessment of the association between TPM3 expression and CESC patient clinical findings

The CESC patients in the TCGA database were divided into two groups according to the level of TPM3 expression (high or low) and clinical characteristics such as age, TNM classification, G classification, and clinical classification were then compared between these subgroups (**Table 1**). This showed a significant association between TPM3 mRNA levels and both histological type and grade ($P = 0.0212$ and $P = 0.0390$, respectively).

TPM3 offers diagnostic utility in CESC

ROC curves were subsequently constructed based on TPM3 expression in CESC (**Figure 2A**), revealing a calculated area under the curve (AUC) value of 0.946, consistent with superior diagnostic utility. Similarly, the AUC values for specific CESC tumor stages were generated, with respective values of 0.948, 0.957, 0.944,

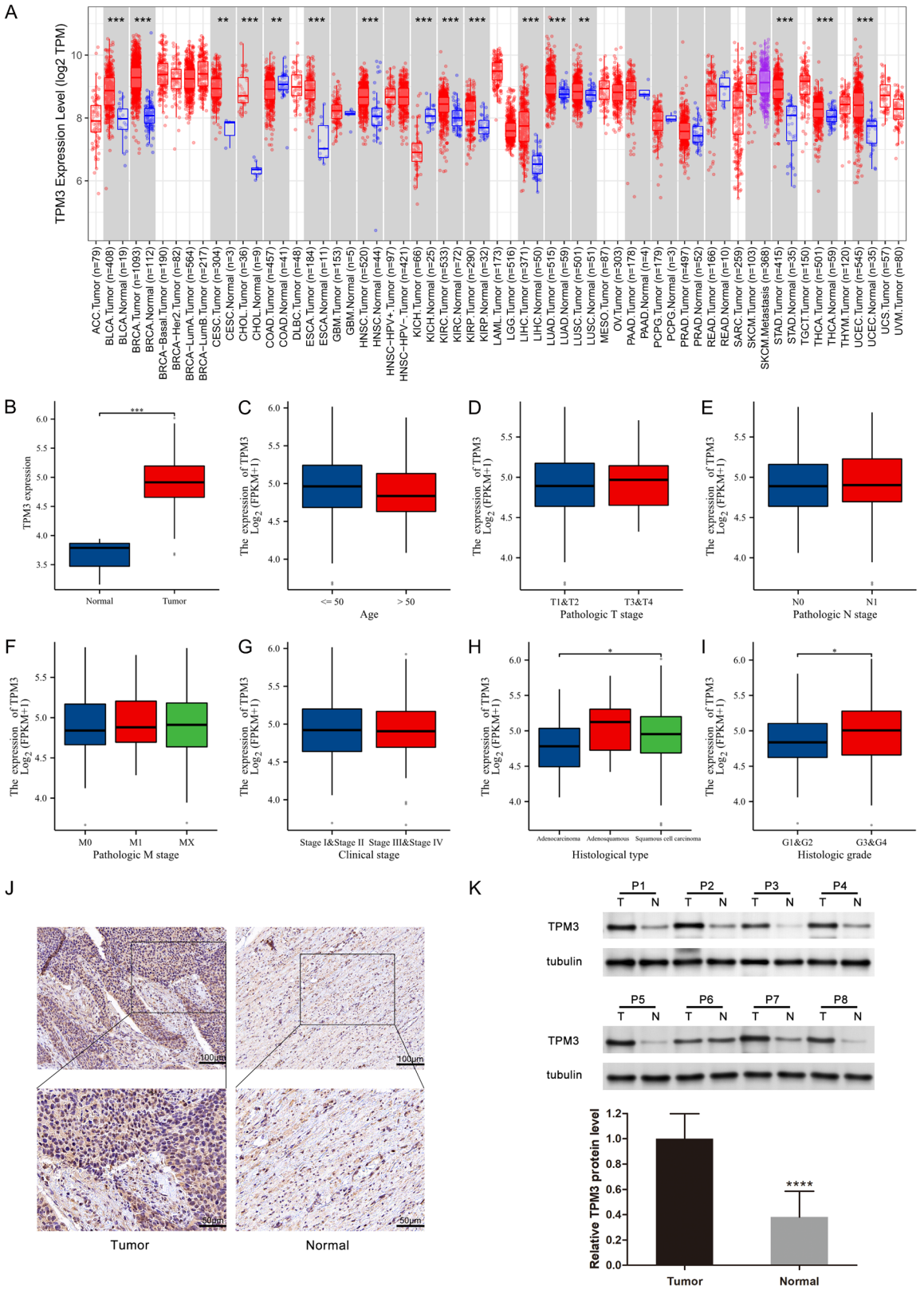

Figure 1. TPM3 mRNA levels in the TCGA database. (A) TPM3 expression was assessed in pan-cancer analyses of tumor and non-tumor samples in the TIMER 2.0 database. (B) TPM3 mRNA expression in CESC and healthy control tissues. (C-I) The associations between TPM3 mRNA expression and clinicopathological parameters of CESC patients, including age, histologic grade, TNM staging, clinical staging, and histological type. (J, K) TPM3 expression was assessed *via* IHC staining (×200 and ×400) (J) and Western immunoblotting (K) in pairs of CESC tumor and paracancerous tissues. **P* < 0.05, ***P* < 0.01, ****P* < 0.001, *****P* < 0.0001.

Table 1. Correlative relationships between the expression of TPM3 and CESC patient clinical characteristics

Characteristics	Variable	No. of patients	TPM3 mRNA expression Characteristics		*P* value
			Low, n (%)	High, n (%)	
Age	≤ 50	188	86 (28.1%)	102 (33.3%)	0.0602
	> 50	118	67 (21.9%)	51 (16.7%)	
Weight	≤ 70	138	70 (25.3%)	68 (24.5%)	0.8568
	> 70	139	69 (24.9%)	70 (25.3%)	
Pathologic T stage	T1	140	71 (29.2%)	69 (28.4%)	0.7932
	T2	72	40 (16.5%)	32 (13.2%)	
	T3	21	11 (4.5%)	10 (4.1%)	
	T4	10	4 (1.6%)	6 (2.5%)	
Pathologic N stage	N0	134	70 (35.9%)	64 (32.8%)	0.8541
	N1	61	31 (15.9%)	30 (15.4%)	
Pathologic M stage	M0	116	63 (24.6%)	53 (20.7%)	0.8191
	M1	11	6 (2.3%)	5 (2%)	
	MX	129	65 (25.4%)	64 (25%)	
Clinical stage	Stage I	162	80 (26.8%)	82 (27.4%)	0.8838
	Stage II	69	33 (11%)	36 (12%)	
	Stage III	46	25 (8.4%)	21 (7%)	
	Stage IV	22	10 (3.3%)	12 (4%)	
Histological type	Adenocarcinoma	47	32 (10.5%)	15 (4.9%)	0.0212
	Adenosquamous	6	2 (0.7%)	4 (1.3%)	
	Squamous cell carcinoma	253	119 (38.9%)	134 (43.8%)	
Histologic grade	G1	19	13 (4.7%)	6 (2.2%)	0.0390
	G2	135	75 (27.4%)	60 (21.9%)	
	G3	119	51 (18.6%)	68 (24.8%)	
	G4	1	0 (0%)	1 (0.4%)	

and 0.919 for stage I, II, III, and IV disease (**Figure 2B-E**). The TPM3 level could also differentiate between early and late CESC stages (AUC: 0.504 for stage I/II vs stage III/IV) (**Figure 2F**).

The prognostic relevance of TPM3 in CESC

The prognostic significance of TPM3 mRNA levels in CESC was further assessed using Kaplan-Meier survival curves, showing that TPM3 overexpression corresponded with poorer OS ($P = 0.045$) (**Figure 3A**). Subgroup analyses also demonstrated a connection between TPM3 expression and OS in younger individuals ($P = 0.02$), N0 stage ($P = 0.034$), and M0 stage patients ($P = 0.015$). However, no correlations were detected in the other subgroups ($P > 0.05$) (**Figure 3B-M**). Univariate analyses indicated that reduced OS was significantly linked with T ($P < 0.001$), N ($P < 0.01$), M ($P < 0.05$), and clinical stage ($P < 0.001$), as well as TPM3 expression ($P < 0.01$). Subsequent multivariate analyses confirmed that the T stage was independently associated with prognosis in CESC patients (hazard ratio = 4.405, $P < 0.05$) (**Table 2**).

Functional verification of the in vitro and in vivo role of TPM3 in CESC

Next, TPM3 silencing was performed in HeLa cells using siRNA and shRNA, and the silencing efficiency was confirmed by RT-qPCR and Western immunoblotting (**Figures 4A** and **5A**). The CCK-8 and colony-forming assays indicated TMP3 knockdown reduced cellular proliferation compared with cells transfected with the control constructs ($P < 0.0001$ and $P < 0.01$, respectively) (**Figure 4B**, **4C**). Loss of TPM3 expression also reduced migration ($P < 0.001$) (**Figure 4D**) and invasion in these cells ($P <$

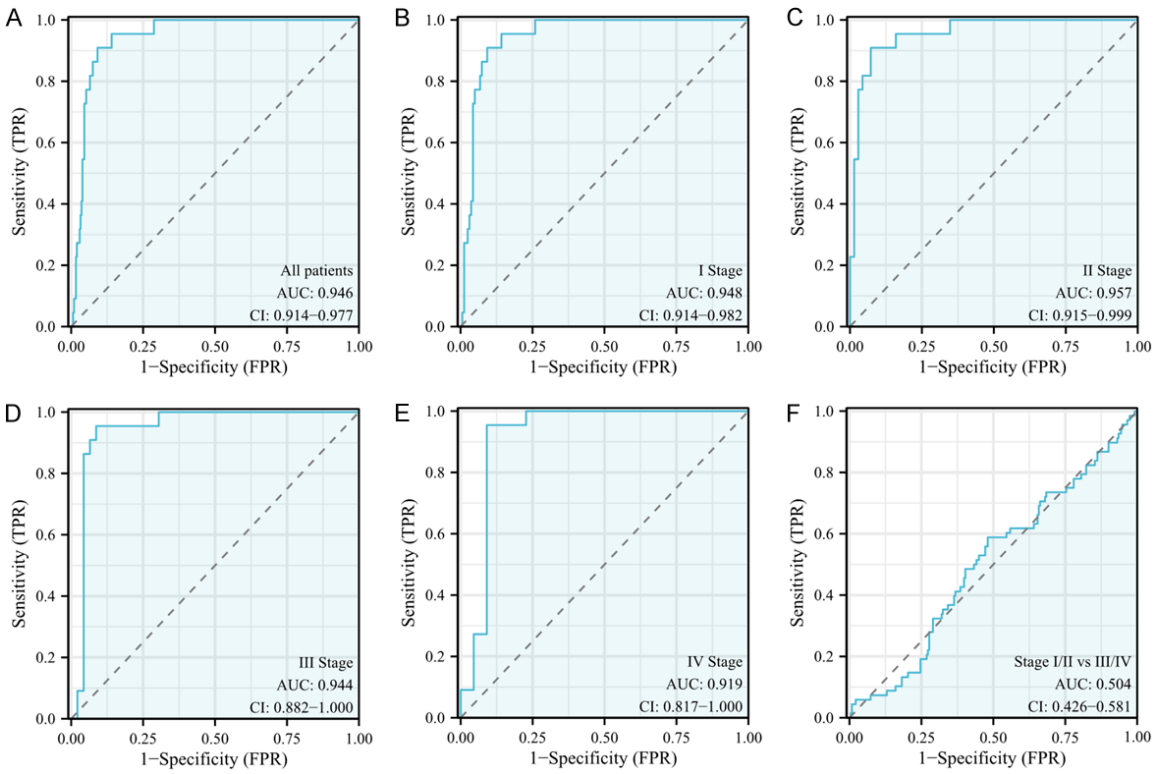

Figure 2. ROC curve analyses of TPM3 in patients with CESC. Comparisons are shown between normal samples and (A) tumors, (B) stage I tumors, (C) stage II tumors, (D) stage III tumors, (E) stage IV tumors, and (F) stage I/II against stage III/IV tumors.

0.001) (**Figure 4E**). Consistently, *in vivo* xenograft experiments revealed that on day 27 after cell implanation, the tumor weights in the sh-NC and sh-TPM3 groups were 355.07 ± 56.20 mg and 183.10 ± 0.61 mg ($P < 0.01$) (**Figure 5B**, **5C**), and the tumor volumes were 611.44 ± 17.66 mm^3 and 331.71 ± 36.56 mm^3 ($P < 0.001$) (**Figure 5D**). Histologic analysis showed a lower degree of malignancy in TPM3 knockdown tumors (**Figure 5E**). Additionally, RT-qPCR and IHC results indicated markedly reduced TPM3 expression in the TPM3-knockdown tumors (**Figure 5F**, **5G**).

Functional analyses of TPM3-related DEGs

Genes associated with TPM3 expression were identified using the LinkedOmics database. Of these, 3011 and 88 DEGs were positively and negatively associated, respectively, with TPM3 expression (**Figure 6A**). The 50 top positively and negatively correlated genes were used to construct a heatmap (**Figure 6B**). KEGG pathway and GO enrichment analyses were used to assess their potential involvement in specific molecular and biological processes. The KEGG analysis demonstrated that the DEGs participated mainly in the PI3K-Akt, HPV infection, focal adhesion, regulation of actin cytoskeleton, and proteoglycans in cancer signaling pathways. The GO analysis revealed that these genes were significant players in processes involving organelle fission, histone modification, covalent chromatin modification, chromosome segregation, nuclear division, and Ras protein signal transduction (**Figure 6C**).

TPM3 levels are associated with tumor immune cell infiltration

Subsequent analyses were carried out to explore the correlation between TPM3 expression and immune cell infiltration of tumors in CESC patients. A positive association was detected between levels of TPM3 and tumor infiltration by aDC ($P = 0.008$), macrophages ($P = 0.035$), neutrophils ($P < 0.001$), NK CD56dim cells ($P = 0.010$), T helper cells ($P = 0.005$), Tgd ($P < 0.001$), and Th2 cells ($P < 0.001$). Conversely, TPM3 expression was inversely correlated with infiltration by NK cells ($P = 0.023$) and pDC ($P = 0.001$) (**Figure 7A**, **7B**). To evalu-

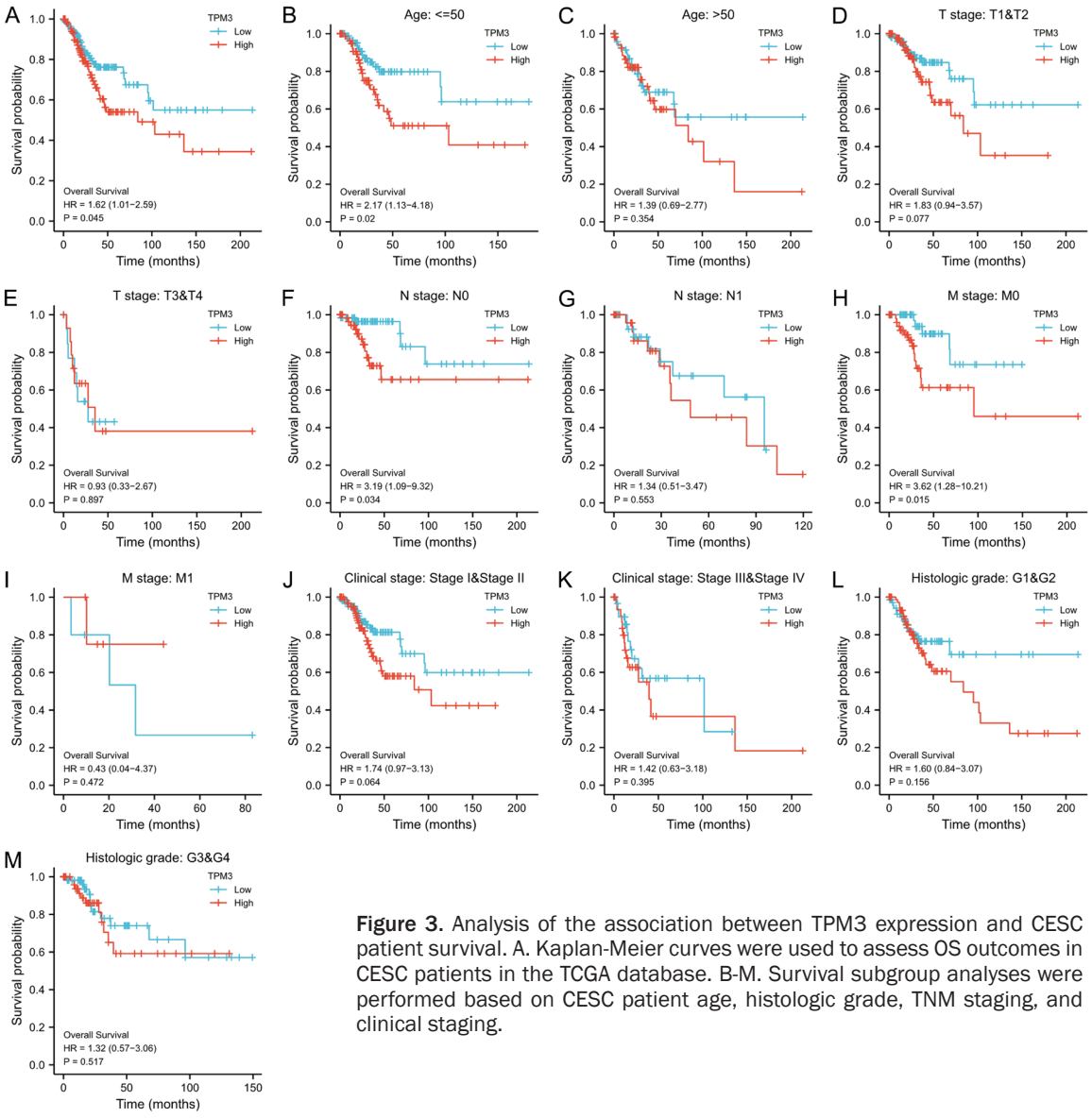

Figure 3. Analysis of the association between TPM3 expression and CESC patient survival. A. Kaplan-Meier curves were used to assess OS outcomes in CESC patients in the TCGA database. B-M. Survival subgroup analyses were performed based on CESC patient age, histologic grade, TNM staging, and clinical staging.

ate the predictive capacity of TPM3 to immunotherapy response, the correlation between TPM3 expression and immune checkpoints was examined. This showed a positive association between TPM3 expression and the expression of CD274 and PDCD1LG2 (P = 4.70e-02 and P = 9.96e-03, respectively) (**Figure 7C**).

TPM3 expression is linked with CESC patient chemotherapeutic sensitivity

Chemotherapy remains the standard approach to treating advanced CESC cases using Bleomycin, Cisplatin, Docetaxel, Gemcitabine, Methotrexate, Mitomycin C, and Paclitaxel. Accordingly, the IC_{50} values for these drugs were compared in different patient groups to gauge chemosensitivity. It was found that patients expressing high TPM3 levels showed reduced IC_{50} values for Bleomycin (P = 1.4e-09), Cisplatin (P = 0.0027), Docetaxel (P = 7.1e-08), Gemcitabine (P = 6.1e-09), Methotrexate (P = 1.4e-05), and Paclitaxel (P = 7.5e-06), whereas these values were not significantly altered for Mitomycin C (P = 0.1) (**Figure 8A-G**).

CESC is associated with altered TPM3 gene methylation

Alterations in the TPM3 gene were next analyzed in CESC patient samples using two databases (**Figure 9B**), revealing a 2.7% prevalence rate of TPM3 genetic alterations (**Figure 9A**).

Table 2. Univariate and multivariate analyses of OS in CESC patients

Characteristics	Univariate analysis			Multivariate analysis		
	Hazard ratio	95% CI	*P* value	Hazard ratio	95% CI	*P* value
Age	1.289	0.810-2.050	0.287			
T stage	3.863	2.072-7.201	< 0.001	4.405	1.005-19.314	< 0.05
N stage	2.844	1.446-5.593	< 0.01	1.779	0.638-4.964	0.271
M stage	3.555	1.187-10.641	< 0.05	0.000	0.000-Inf	0.998
Clinical stage	2.369	1.457-3.854	< 0.001	0.527	0.094-2.972	0.468
Histological type	1.033	0.543-1.969	0.920			
Histologic grade	0.866	0.514-1.459	0.589			
TPM3	2.147	1.205-3.826	< 0.01	2.646	0.795-8.802	0.113

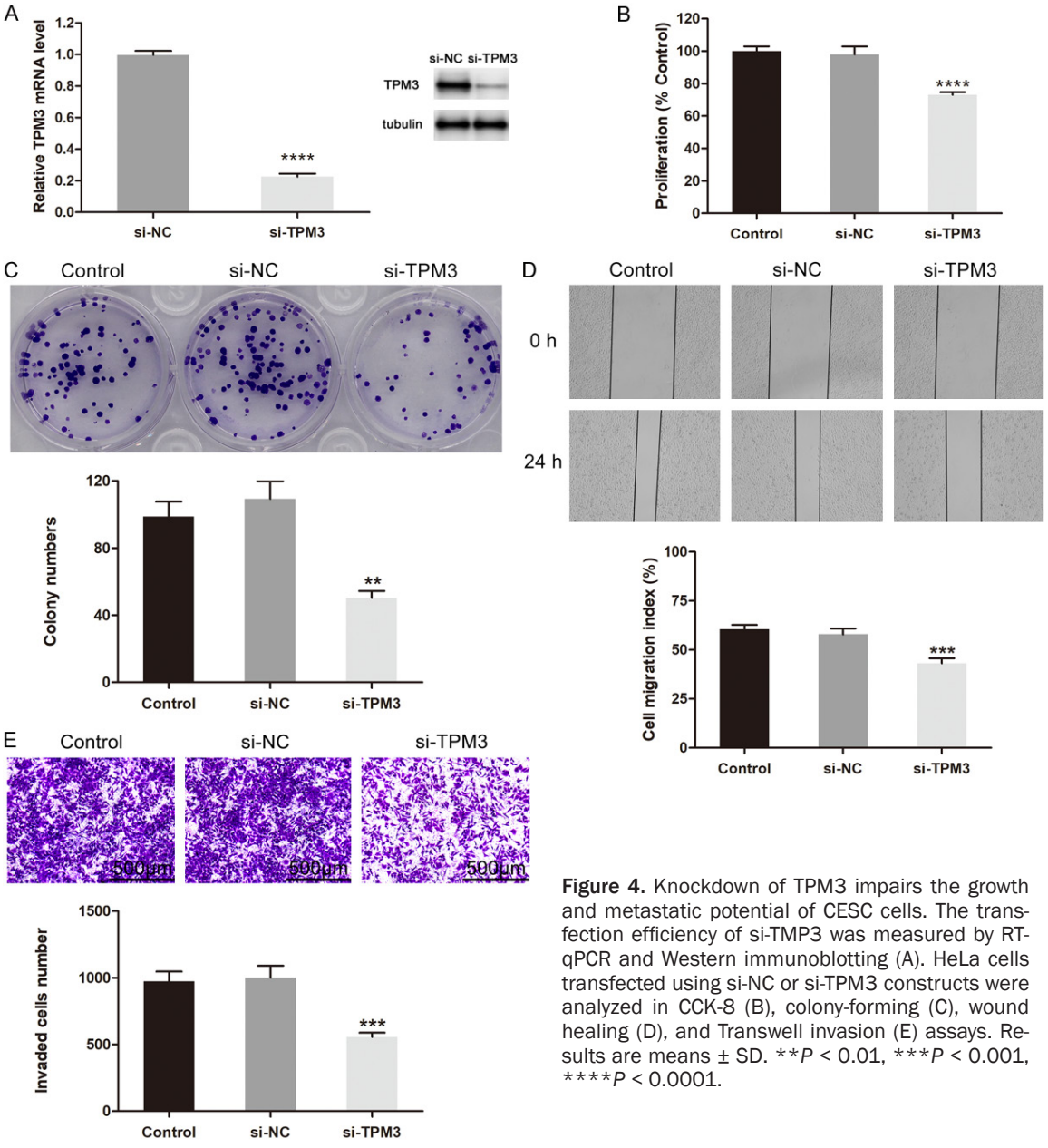

Figure 4. Knockdown of TPM3 impairs the growth and metastatic potential of CESC cells. The transfection efficiency of si-TMP3 was measured by RT-qPCR and Western immunoblotting (A). HeLa cells transfected using si-NC or si-TPM3 constructs were analyzed in CCK-8 (B), colony-forming (C), wound healing (D), and Transwell invasion (E) assays. Results are means ± SD. ***P* < 0.01, ****P* < 0.001, *****P* < 0.0001.

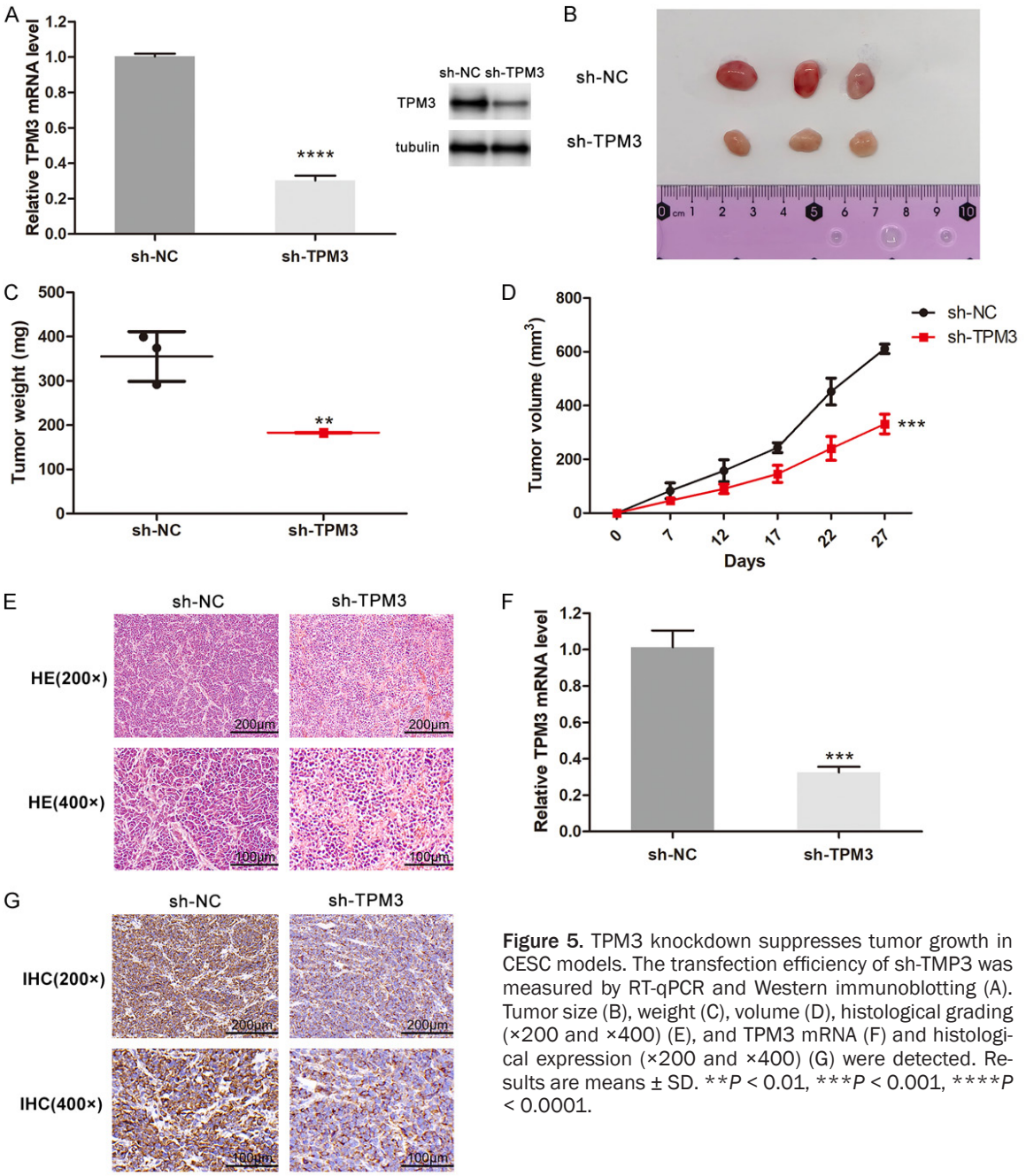

Figure 5. TPM3 knockdown suppresses tumor growth in CESC models. The transfection efficiency of sh-TMP3 was measured by RT-qPCR and Western immunoblotting (A). Tumor size (B), weight (C), volume (D), histological grading (×200 and ×400) (E), and TPM3 mRNA (F) and histological expression (×200 and ×400) (G) were detected. Results are means ± SD. $^{**}P < 0.01$, $^{***}P < 0.001$, $^{****}P < 0.0001$.

These were found to be unrelated to patient survival outcomes when comparing individuals that did and did not harbor these mutations ($P = 0.319$) (**Figure 9C**). Lastly, TPM3 methylation was explored using the MethSurv tool to examine the prognostic relevance of specific CpG residues. This ultimately identified 17 key CpG residues, the most highly methylated of which was cg03830929 (**Figure 9D**). Notably, 5 of these CpG residues were found to be related to CESC patient prognosis. Specifically, high levels of cg00155429 (HR = 1.67, $P = 0.0369$), cg13188812 (HR = 1.994, $P = 0.0050$), cg13740187 (HR = 1.907, $P = 0.0358$), and cg25107608 (HR = 1.77, $P = 0.0202$) methylation were tied to poorer CESC patient OS (**Table 3**). In contrast, high levels of cg10890570 (HR = 0.502, $P = 0.0068$) led to better CESC patient OS.

Discussion

With the rapid development of genome sequencing technology, the cost of sequencing has decreased, and the sequencing throughput

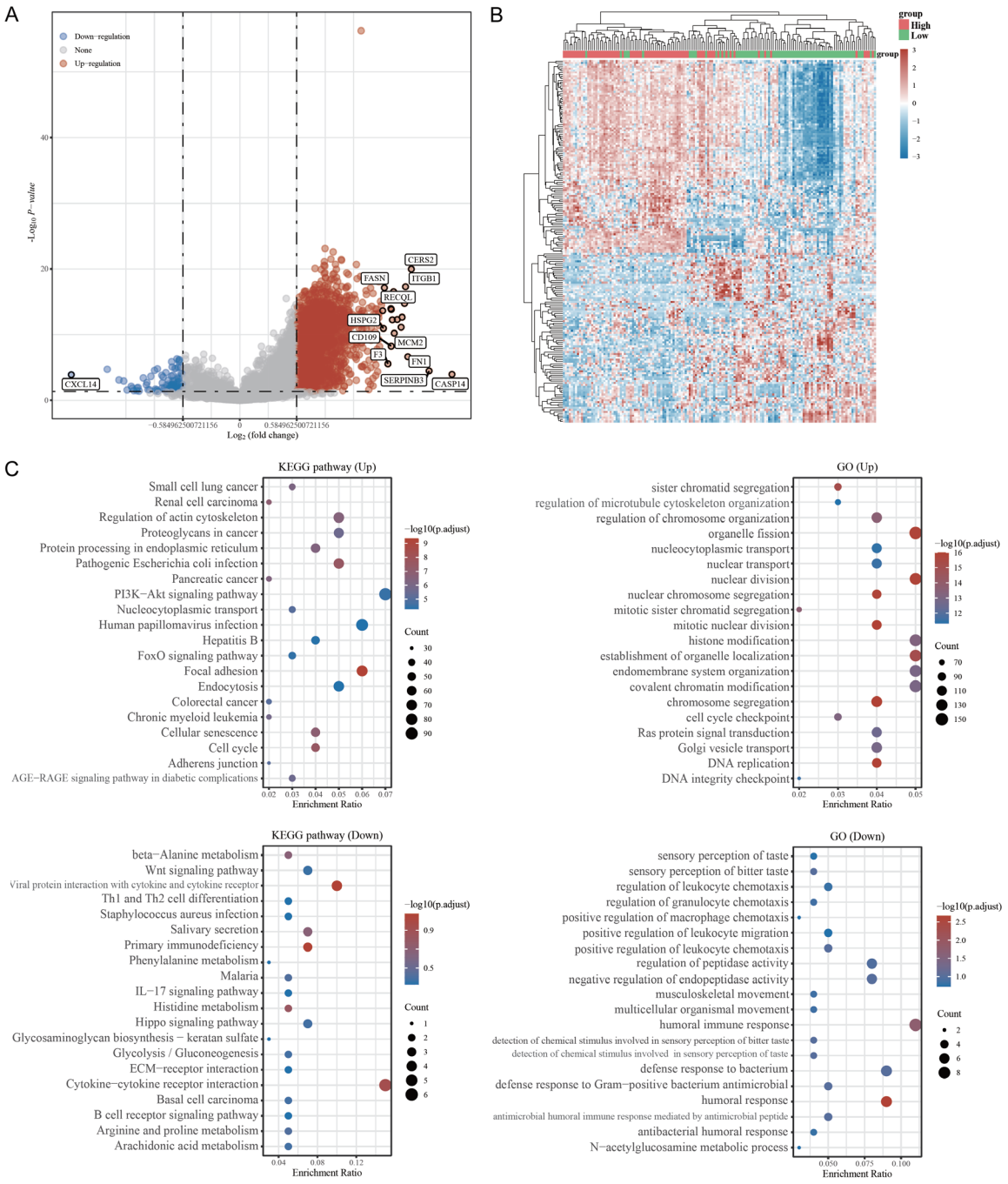

Figure 6. Enrichment analyses of TPM3-associated DEGs. A. Volcano plot of the identified DEGs. Upregulated genes are shown in red and downregulated genes in blue. B. Heatmap of DEGs with upregulated genes shown in red and downregulated genes in blue. C. DEG KEGG and GO enrichment analyses.

has increased, leading to the wide application of next-generation sequencing. The reliable transformation of this big-data information is of inestimable clinical significance for the guidance of patient treatment [13]. Nowadays, with the help of various bioinformatics tools, there has been an increase in the number of reported candidate molecules with potential prognostic value for CESC [14, 15]. Biomarkers with prognostic value can monitor tumor recurrence and evaluate prognosis, which is conducive to the individualized treatment of CESC patients.

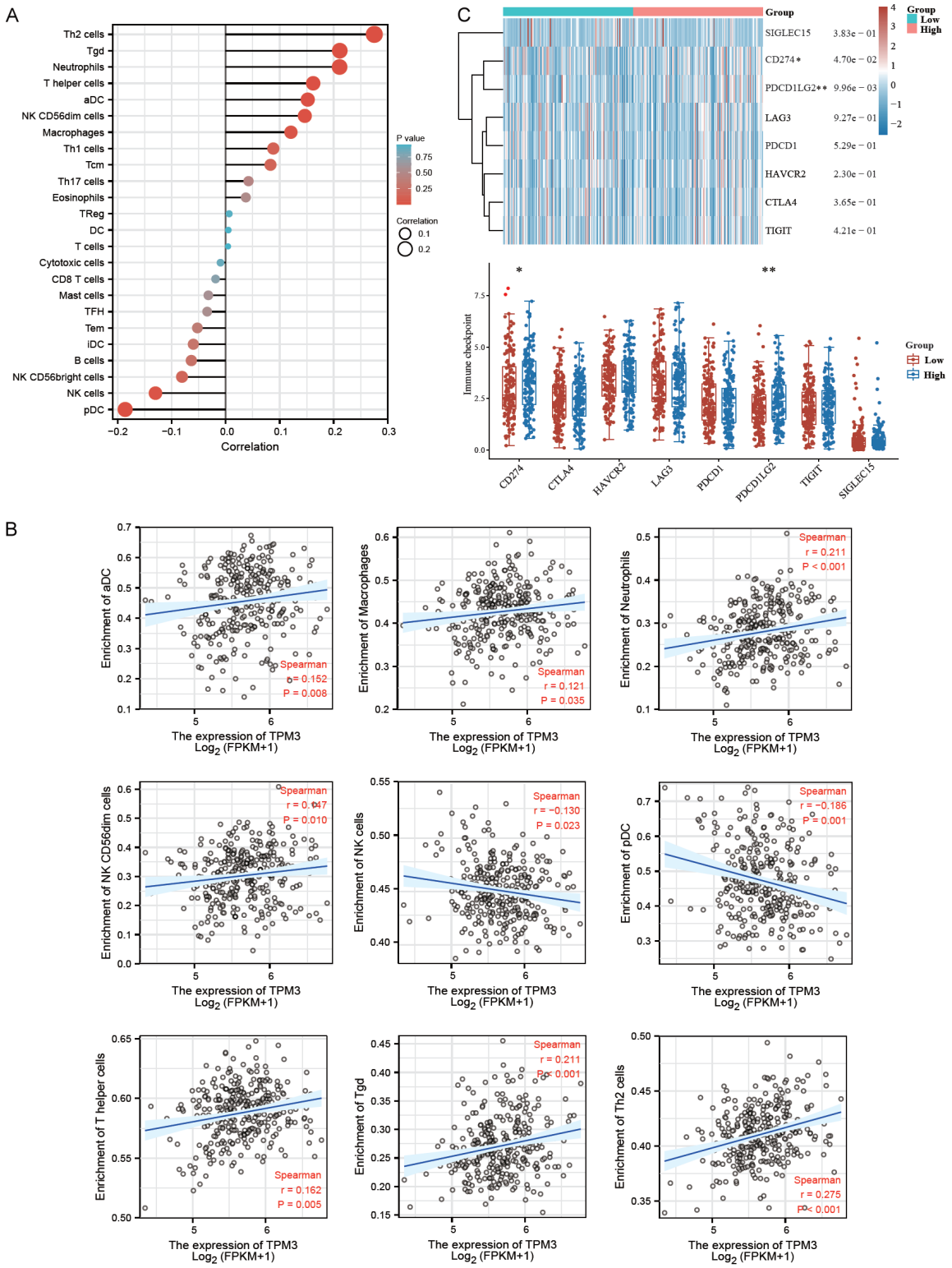

Figure 7. TME immune cell infiltration analyses. A. A forest plot. B. Spearman correlation analyses. C. The expression of immune checkpoint markers was assessed in groups of patients expressing low and high levels of TPM3. *P < 0.05, **P < 0.01.

The present study used comprehensive data mining and bioinformatics analyses to determine the potential prognostic and therapeutic value of potential biomarkers for CESC.

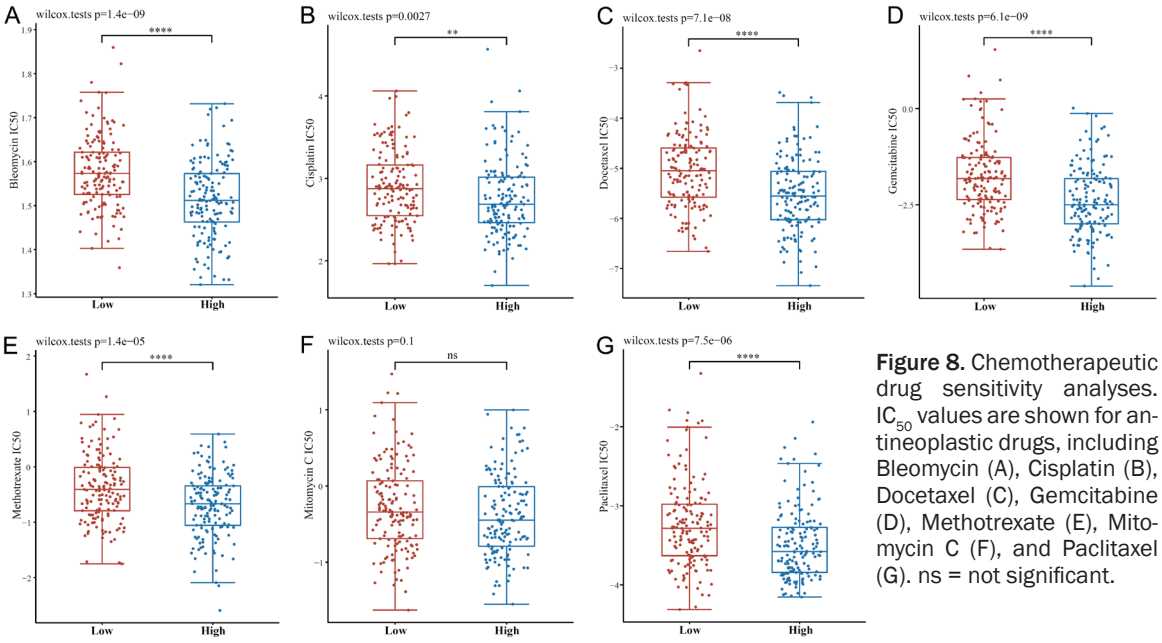

Figure 8. Chemotherapeutic drug sensitivity analyses. IC_{50} values are shown for antineoplastic drugs, including Bleomycin (A), Cisplatin (B), Docetaxel (C), Gemcitabine (D), Methotrexate (E), Mitomycin C (F), and Paclitaxel (G). ns = not significant.

The EMT is a process that occurs under specific physiological or pathological circumstances in which polar epithelial cells transform into highly active, mobile mesenchymal cells that can navigate freely within cellular matrices [16]. There is a strong correlation between the EMT and cancer cell invasion and metastasis. In early-stage tumors, the onset of the EMT triggers alterations in cell structure and the expression levels of intercellular junction molecules, notably E-cadherin. As E-cadherin functions as a cell adhesion molecule, its loss removes an obstacle to cell migration and metastasis and is thus an initial step in the progression of tumor cell de-differentiation and invasion [17].

Recent research has shown that TPM3 is involved in the genesis and development of tumors in non-muscle tissues. Choi et al. and Tao et al. confirmed that TPM3 overexpression could facilitate cancer invasion and metastasis in primary liver cancer and glioma, respectively, and was related to the upregulation of EMT-associated signaling [18, 19]. Elevated expression of TPM3 can also significantly increase the risk of primary liver cancer [20]. Glioma and liver cancer patients with high expression levels of TPM3 often have poor prognosis [8, 19]. In hepatocellular carcinoma cell lines, amplification of TPM3 can lead to an upregulation of the EMT and downregulation of E-cadherin, ultimately leading to the migration and invasion of hepatocellular carcinoma and worse prognosis [18].

Chromosomal structural translocations, ensuing gene rearrangements, and fusions are acknowledged as pivotal steps in the activation of proto-oncogenes. TPM3 can form fusion genes with other genes, inducing alterations in the cytoskeleton, thereby facilitating cell movement and metastasis and ultimately promoting tumor progression [21]. The fusion gene TPM3-ALK, a consequence of chromosomal translocation (1, 2) (q25, p23), has been associated with the development of anaplastic large-cell lymphoma [22, 23]. In NIH3T3 cells, the TPM3-ALK fusion gene stimulated an increase in both cell proliferation and invasive capacities [24]. A mouse model of B-cell leukemia also demonstrated the presence of the TPM3-ALK fusion gene, the effects of which could be mitigated by an ALK inhibitor [25]. TPM3/NTRK1 and TPM3/PDGFRB gene recombinations have been implicated in the pathogenesis of papillary thyroid carcinoma and chronic eosinophilic leukemia, respectively [26, 27]. Furthermore, TPM3 has been shown to interact with various genes such as those encoding receptor tyrosine kinases, platelet-derived growth factor receptor beta, anaplastic lymphoma receptor tyrosine kinase, and neurotrophic receptor tyrosine kinase 1 to form fusion genes, thereby contributing to tumor development [28-30].

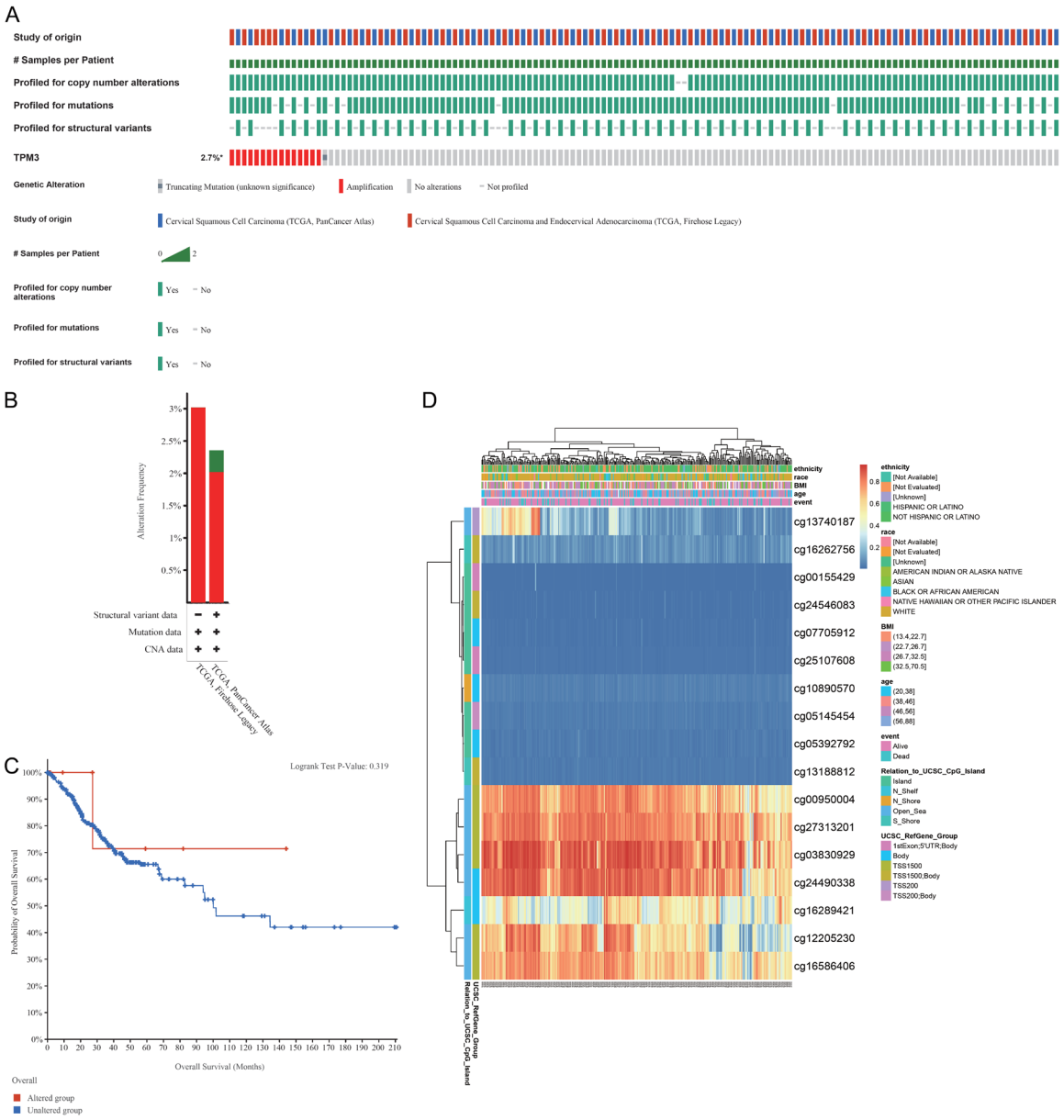

Figure 9. Changes in TPM3 genetic sequences and methylation status in CESC patients. A. A visual summary of TPM3 alterations produced using OncoPrint. B. A summary of CESC-related TPM3 variations from the TCGA, Firehose Legacy, and TCGA PanCancer Atlas databases. C. The OS of patients that did and did not harbor alterations in the TPM3 gene sequence was compared with Kaplan-Meier plots. D. TPM3 methylation and expression levels were assessed.

The above findings underscore the need to assess TPM3 as a regulator of oncogenesis, tumor progression, and prognostic outcomes. Therefore, we explored the role of TPM3 in CESC in this research, which has not been previously undertaken. TPM3 overexpression was detected in CESC tumors relative to healthy tissues and was verified in a separate set of clinical samples. TPM3 levels could also effectively differentiate among stages of CESC, consistent with its biomarker utility. High TPM3 levels were also associated with poorer patient OS, and *in vitro* and xenograft experiments supported the role of TPM3 as a pro-oncogenic factor, further solidifying its importance in this cancerous setting.

Table 3. The relationship between hypermethylation levels and CESC patient prognostic outcomes

Name	HR	*P* value
1st Exon; 5'UTR; Body-Island-cg00155429	1.67	0.0369
TSS1500-Open_Sea-cg00950004	0.677	0.1922
TSS1500-Open_Sea-cg03830929	0.753	0.3282
TSS200; Body-Island-cg05145454	0.668	0.0951
Body-Island-cg05392792	1.199	0.4450
Body-Island-cg07705912	1.183	0.4776
Body-N_Shore-cg10890570	0.502	0.0068
TSS1500-Open_Sea-cg12205230	0.689	0.1192
TSS1500; Body-S_Shore-cg13188812	1.994	0.0050
TSS200-Open_Sea-cg13740187	1.907	0.0358
TSS1500; Body-S_Shore-cg16262756	1.162	0.6260
Body-N_Shelf-cg16289421	0.636	0.0599
TSS1500-Open_Sea-cg16586406	0.789	0.4147
Body-Open_Sea-cg24490338	0.798	0.3496
TSS1500; Body-Island-cg24546083	0.658	0.1031
1st Exon; 5'UTR; Body-Island-cg25107608	1.77	0.0202
TSS1500-Open_Sea-cg27313201	1.441	0.2219

Key co-expressed genes were identified and subjected to functional enrichment analyses to better define the functional roles of TPM3 in the progression of CESC. Significant enrichment was observed in several KEGG pathways, including the PI3K-Akt pathway. As one of the important signal transduction pathways in cells, the PI3K-Akt signaling pathway plays a key role in promoting cell proliferation and inhibiting apoptosis *in vivo* by affecting the activation status of various downstream effectors, which is closely related to the occurrence and development of various malignancies [31]. Focal adhesions are complex collections of plasma membrane-related macromolecules that connect the actin cytoskeleton to integrins on the cell surface and establish links to the extracellular matrix (ECM). Focal adhesions generate traction and convert signals to drive cell migration through adhesion and changes in molecular interactions during cell maturation. The loss or change of any of the above processes will reduce the ability of cells to remain in place, one of the most important factors leading to tumor metastasis [32]. Proteoglycans are important molecular effectors on the cell surface and the microenvironment surrounding cells and belong to the non-collagen components of the ECM. They can interact with receptors and ligands that regulate carcinogenesis and angiogenesis and participate in tumorigenesis and angiogenesis [33]. Besides, HPV infection is the most important exposure factor associated with CESC. The processes identified in the GO analysis were related to epigenetic modification and changes in chromosome structure. We speculate that this may be involved in epigenetic abnormalities in the development of CESC and the TPM3 fusion gene due to variations in chromosomal structure. Accordingly, high TPM3 expression levels may partly shape CESC progression through these pathways.

In recent years, the tumor microenvironment (TME) has become a hot research topic in cancer research. Immune cell subsets, including T cells, macrophages, NK cells, and dendritic cells, interact with tumor cells either according to their functions or through the expression and secretion of inhibitory molecules to maintain the immunosuppressive character of the TME, thereby affecting the occurrence, development, invasion, and metastasis of tumors. Therefore, it is of great significance to study the TME of CESC. Focusing on the components and inhibitory characteristics of the CESC TME is expected to provide new ideas and directions for the immunotherapy of CESC [34]. Here, TPM3 expression was found to be positively correlated with tumor infiltration by aDC, macrophages, neutrophils, NK CD56dim cells, T helper cells, Tgd, and Th2 cells, and negatively correlated with NK cells and pDC. In addition, patients showing TPM3 overexpression had upregulated expression of the classical immune checkpoint molecules CD274 and PDCD1LG2. Accordingly, we speculate that TPM3 expression is highly correlated with immune infiltration in the TME of CESC. When TPM3 is abnormally expressed, it may disrupt the immune homeostasis of the TME, resulting in tumor immune escape.

Unrestrained tumor cell growth is a hallmark of cancer that results from oncogenic driver mutations. TPM3 mutations were detected in just 2.7% of all CESC patients. However, recent studies have found that epigenetic changes in gene methylation also have significant value as cancer-related biomarkers, with many DNA-related research findings having aided efforts

to diagnose, evaluate, or treat specific tumor types [35, 36]. Accordingly, key CpG residues that were methylated in a manner associated with CESC patient prognosis were identified in the present study.

In summary, in this study, TPM3 expression was identified as a key biomarker associated with CESC patient outcomes, with especial relevance in the context of immunotherapeutic treatment. These results will provide a valuable basis for further efforts to define the major pathways governing CESC tumor malignancy and progression, supporting the development of novel targeted therapies.

Disclosure of conflict of interest

None.

Address correspondence to: Hong-Dao Qu, Department of Radiation Oncology, The Second Hospital of Jilin University, Changchun 130041, Jilin, P. R. China. E-mail: quhd2716@163.com

References

[1] Bray F, Ferlay J, Soerjomataram I, Siegel RL, Torre LA and Jemal A. Global cancer statistics 2018: GLOBOCAN estimates of incidence and mortality worldwide for 36 cancers in 185 countries. CA Cancer J Clin 2018; 68: 394-424.

[2] Cohen PA, Jhingran A, Oaknin A and Denny L. Cervical cancer. Lancet 2019; 393: 169-182.

[3] Arbyn M, Weiderpass E, Bruni L, de Sanjose S, Saraiya M, Ferlay J and Bray F. Estimates of incidence and mortality of cervical cancer in 2018: a worldwide analysis. Lancet Glob Health 2020; 8: e191-e203.

[4] Gunning PW, Hardeman EC, Lappalainen P and Mulvihill DP. Tropomyosin - master regulator of actin filament function in the cytoskeleton. J Cell Sci 2015; 128: 2965-2974.

[5] Lees JG, Bach CT and O'Neill GM. Interior decoration: tropomyosin in actin dynamics and cell migration. Cell Adh Migr 2011; 5: 181-186.

[6] Schreckenbach T, Schroder JM, Voit T, Abicht A, Neuen-Jacob E, Roos A, Bulst S, Kuhl C, Schulz JB, Weis J and Claeys KG. Novel TPM3 mutation in a family with cap myopathy and review of the literature. Neuromuscul Disord 2014; 24: 117-124.

[7] Yang J, Dong L, Du H, Li XB, Liang YX and Liu GR. ALK-TPM3 rearrangement in adult renal cell carcinoma: a case report and literature review. Diagn Pathol 2019; 14: 112.

[8] Lam CY, Yip CW, Poon TC, Cheng CK, Ng EW, Wong NC, Cheung PF, Lai PB, Ng IO, Fan ST and Cheung ST. Identification and characterization of tropomyosin 3 associated with granulin-epithelin precursor in human hepatocellular carcinoma. PLoS One 2012; 7: e40324.

[9] Tian Z, Zhao J and Wang Y. The prognostic value of TPM1-4 in hepatocellular carcinoma. Cancer Med 2022; 11: 433-446.

[10] Sohn SH, Sul HJ, Kim B, Kim BJ, Kim HS and Zang DY. TRK inhibitors block NFKB and induce NRF2 in TRK fusion-positive colon cancer. J Cancer 2021; 12: 6356-6362.

[11] Chen S, Shen Z, Gao L, Yu S, Zhang P, Han Z and Kang M. TPM3 mediates epithelial-mesenchymal transition in esophageal cancer via MMP2/MMP9. Ann Transl Med 2021; 9: 1338.

[12] Zhu YC, Liao XH, Wang WX, Xu CW, Zhuang W, Wei JG and Du KQ. Dual drive coexistence of EML4-ALK and TPM3-ROS1 fusion in advanced lung adenocarcinoma. Thorac Cancer 2018; 9: 324-327.

[13] Goodwin S, McPherson JD and McCombie WR. Coming of age: ten years of next-generation sequencing technologies. Nat Rev Genet 2016; 17: 333-351.

[14] Zhao K, Yi Y, Ma Z and Zhang W. INHBA is a prognostic biomarker and correlated with immune cell infiltration in cervical cancer. Front Genet 2021; 12: 705512.

[15] Liu H, Xu R, Gao C, Zhu T, Liu L, Yang Y, Zeng H, Huang Y and Wang H. Metabolic molecule PLA2G2D is a potential prognostic biomarker correlating with immune cell infiltration and the expression of immune checkpoint genes in cervical squamous cell carcinoma. Front Oncol 2021; 11: 755668.

[16] Loh CY, Chai JY, Tang TF, Wong WF, Sethi G, Shanmugam MK, Chong PP and Looi CY. The E-cadherin and N-cadherin switch in epithelial-to-mesenchymal transition: signaling, therapeutic implications, and challenges. Cells 2019; 8: 1118.

[17] Wong SHM, Fang CM, Chuah LH, Leong CO and Ngai SC. E-cadherin: its dysregulation in carcinogenesis and clinical implications. Crit Rev Oncol Hematol 2018; 121: 11-22.

[18] Choi HS, Yim SH, Xu HD, Jung SH, Shin SH, Hu HJ, Jung CK, Choi JY and Chung YJ. Tropomyosin3 overexpression and a potential link to epithelial-mesenchymal transition in human hepatocellular carcinoma. BMC Cancer 2010; 10: 122.

[19] Tao T, Shi Y, Han D, Luan W, Qian J, Zhang J, Wang Y and You Y; Chinese Glioma Cooperative Group (CGCG). TPM3, a strong prognosis predictor, is involved in malignant progression through MMP family members and EMT-like activators in gliomas. Tumour Biol 2014; 35: 9053-9059.

[20] Kim TM, Yim SH, Shin SH, Xu HD, Jung YC, Park CK, Choi JY, Park WS, Kwon MS, Fiegler H, Cart-

er NP, Rhyu MG and Chung YJ. Clinical implication of recurrent copy number alterations in hepatocellular carcinoma and putative oncogenes in recurrent gains on 1q. Int J Cancer 2008; 123: 2808-2815.
[21] Armstrong F, Lamant L, Hieblot C, Delsol G and Touriol C. TPM3-ALK expression induces changes in cytoskeleton organisation and confers higher metastatic capacities than other ALK fusion proteins. Eur J Cancer 2007; 43: 640-646.
[22] Lamant L, Dastugue N, Pulford K, Delsol G and Mariame B. A new fusion gene TPM3-ALK in anaplastic large cell lymphoma created by a (1;2)(q25;p23) translocation. Blood 1999; 93: 3088-3095.
[23] Rosenwald A, Ott G, Pulford K, Katzenberger T, Kuhl J, Kalla J, Ott MM, Mason DY and Muller-Hermelink HK. t(1;2)(q21;p23) and t(2;3)(p23;q21): two novel variant translocations of the t(2;5)(p23;q35) in anaplastic large cell lymphoma. Blood 1999; 94: 362-364.
[24] Armstrong F, Duplantier MM, Trempat P, Hieblot C, Lamant L, Espinos E, Racaud-Sultan C, Allouche M, Campo E, Delsol G and Touriol C. Differential effects of X-ALK fusion proteins on proliferation, transformation, and invasion properties of NIH3T3 cells. Oncogene 2004; 23: 6071-6082.
[25] Giuriato S, Foisseau M, Dejean E, Felsher DW, Al Saati T, Demur C, Ragab A, Kruczynski A, Schiff C, Delsol G and Meggetto F. Conditional TPM3-ALK and NPM-ALK transgenic mice develop reversible ALK-positive early B-cell lymphoma/leukemia. Blood 2010; 115: 4061-4070.
[26] Butti MG, Bongarzone I, Ferraresi G, Mondellini P, Borrello MG and Pierotti MA. A sequence analysis of the genomic regions involved in the rearrangements between TPM3 and NTRK1 genes producing TRK oncogenes in papillary thyroid carcinomas. Genomics 1995; 28: 15-24.
[27] Rosati R, La Starza R, Luciano L, Gorello P, Matteucci C, Pierini V, Romoli S, Crescenzi B, Rotoli B, Martelli MF, Pane F and Mecucci C. TPM3/PDGFRB fusion transcript and its reciprocal in chronic eosinophilic leukemia. Leukemia 2006; 20: 1623-1624.
[28] Galea LA, Hildebrand MS, Witkowski T, Joy C, McEvoy CR, Hanegbi U and Aga A. ALK-rearranged renal cell carcinoma with TPM3:ALK gene fusion and review of the literature. Virchows Arch 2023; 482: 625-633.
[29] Gatalica Z, Xiu J, Swensen J and Vranic S. Molecular characterization of cancers with NTRK gene fusions. Mod Pathol 2019; 32: 147-153.
[30] Li Z, Yang R, Zhao J, Yuan R, Lu Q, Li Q and Tse W. Molecular diagnosis and targeted therapy of a pediatric chronic eosinophilic leukemia patient carrying TPM3-PDGFRB fusion. Pediatr Blood Cancer 2011; 56: 463-466.
[31] Alzahrani AS. PI3K/Akt/mTOR inhibitors in cancer: at the bench and bedside. Semin Cancer Biol 2019; 59: 125-132.
[32] Le Coq J, Acebron I, Rodrigo Martin B, Lopez Navajas P and Lietha D. New insights into FAK structure and function in focal adhesions. J Cell Sci 2022; 135: jcs259089.
[33] Karagiorgou Z, Fountas PN, Manou D, Knutsen E and Theocharis AD. Proteoglycans determine the dynamic landscape of EMT and cancer cell stemness. Cancers (Basel) 2022; 14: 5328.
[34] Lv B, Wang Y, Ma D, Cheng W, Liu J, Yong T, Chen H and Wang C. Immunotherapy: reshape the tumor immune microenvironment. Front Immunol 2022; 13: 844142.
[35] Lau CE and Robinson O. DNA methylation age as a biomarker for cancer. Int J Cancer 2021; 148: 2652-2663.
[36] Constancio V, Nunes SP, Henrique R and Jeronimo C. DNA methylation-based testing in liquid biopsies as detection and prognostic biomarkers for the four major cancer types. Cells 2020; 9: 624.